Linear and nonlinear optics of surface-plasmon whispering-gallery modes

Igor I. Smolyaninov and Christopher C. Davis
Department of Electrical and Computer Engineering, University of Maryland, College Park, Maryland 20742, USA
(Received 19 December 2003; revised manuscript received 18 March 2004; published 28 May 2004)

Experimental and theoretical studies of linear and nonlinear optics of surface plasmon whispering gallery modes have been performed. These modes have been observed in dielectric microdroplets on the metal surfaces which support surface plasmon propagation. The plasmons have been shown to exhibit critical behavior near some surface just inside the droplet edge, where the effective refractive index seen by the surface plasmons appears to be extremely large.

DOI: 10.1103/PhysRevB.69.205417 PACS number(s): 78.67.−n, 04.70.Bw

I. INTRODUCTION

The emerging field of nanophotonics is based on the optics of surface plasmon-polaritons.[1] Until recently most work on this basically two-dimensional (2D) optics was concentrated on showing that in two dimensions one can successfully perform all the same optical experiments and build devices, which were previously performed and/or built in regular three-dimensional optics. Experiments with individual metal nanoparticles and nanoparticle chains, in which one can produce field localization and energy transport on sub-diffraction-limited scale remain an exception. However, it was understood that these are not 2D situations, and the perception of 2D optics of surface plasmon-polaritons as a reduced copy of 3D optics prevails at the moment.

In this paper we are going to demonstrate a set of phenomena, which are based on an overlooked fundamental distinction between 2D and 3D optics. In 3D optics the range of refractive indices of transparent materials is limited in the visible range by values of the order of 2.5. Below we will show that the effective refractive index n_{eff} of a transparent dielectric droplet on the metal surface which supports plasmon-polariton propagation may reach much larger values, which leads one to a host of unusual 2D optical devices and phenomena. For example, the diffraction limit of a plasmon-polariton field focusing by a transparent dielectric droplet shifts down to nanometer scale $\lambda/2n_{eff}$ values, which theoretically makes possible a 2D far-field optical microscopy with a similar-scale resolution. This issue will be addressed in a separate paper. On the other hand, large effective refractive index of a dielectric droplet leads to very efficient trapping of surface plasmon-polariton field in the whispering gallery modes, which may lead to new understanding of such phenomena as surface enhanced Raman scattering (SERS).

Let us consider in detail the dispersion law of a surface plasmon (SP), which propagates along the metal-dielectric interface. The SP field decays exponentially both inside the metal and the dielectric. Inside the dielectric the decay exponent is roughly equal to the SP wave vector. As a first step let us assume that both metal and dielectric completely fill the respective $z<0$ and $z>0$ half-spaces. In such a case the dispersion law can be written as[1,2]

$$k^2=\frac{\omega^2}{c^2}\frac{\epsilon_d\epsilon_m(\omega)}{\epsilon_d+\epsilon_m(\omega)}, \tag{1}$$

where we will assume that $\epsilon_m=1-\omega_p^2/\omega^2$ according to the Drude model, and ω_p is the plasma frequency of the metal. This dispersion law is shown in Fig. 1(b) for the cases of metal-vacuum and metal-dielectric interfaces. It starts as a

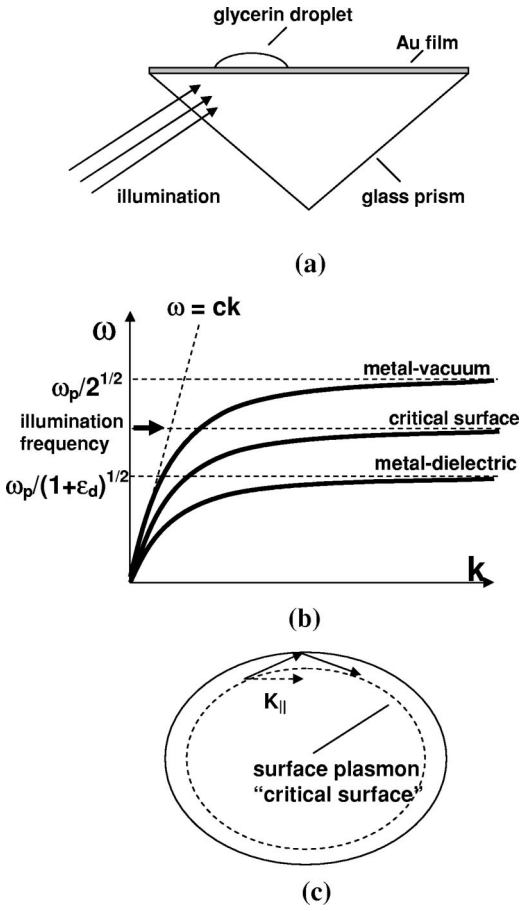

FIG. 1. (a) Experimental geometry of surface plasmon whispering gallery mode observation. (b) Surface plasmon dispersion laws for the cases of metal-vacuum interface far from the droplet, for metal-dielectric interface deep inside the droplet, and somewhere near the droplet edge. (c) A surface plasmon trapped inside a droplet near the critical surface: The projection of surface plasmon momentum parallel to the droplet edge must be conserved. Due to extremely large effective refractive index near the droplet edge surface plasmons experience total internal reflection at almost any angle of incidence.

''light line'' in the respective dielectric at low frequencies and approaches asymptotically $\omega = \omega_p/(1+\epsilon_d)^{1/2}$ at very large wave vectors. The latter frequency corresponds to the so-called surface plasmon resonance. Under the surface plasmon resonance conditions both phase and group velocity of the SPs is zero, and the surface charge and the normal component of the electric field diverge. Since at every wave vector the SP dispersion law is located to the right of the ''light line,'' the SP's of the plane metal-dielectric interface are decoupled from the free-space photons due to the momentum conservation law.

If a curved dielectric object [say, a droplet like in Fig. 1(a)] is placed on the metal surface, the SP dispersion law will be a function of the local thickness of the droplet and the local value of its dielectric constant, which may or may not be constant throughout the droplet. Deep inside the droplet far from its edges the SP dispersion law will look similar to the case of a metal-dielectric interface, whereas, near the edges (where the dielectric is thinner) it will approach the SP dispersion law for the metal-vacuum interface. The behavior of the SP dispersion law for the range of intermediate thicknesses is somewhat more complicated: the dispersion curve reaches a broad maximum followed by a very slow decline towards $\omega = \omega_p/(1+\epsilon_d)^{1/2}$ at $k \to \infty$. However, this behavior at very large k gets complicated by the effects of spatial dispersion, which bends the dispersion curve up again. In order to avoid these complications we may assume that the spatial distribution of the dielectric constant ϵ_d inside the droplet is chosen by an experimenter such that at each illumination frequency in the range between $\omega_p/(1+\epsilon_d)^{1/2}$ and $\omega_p/2^{1/2}$ there will be a closed linear boundary inside the droplet for which the surface plasmon resonance conditions are satisfied [Figs. 1(b) and 1(c)].

Let us show qualitatively that in the frequency range between $\omega_p/(1+\epsilon_d)^{1/2}$ and $\omega_p/2^{1/2}$ the described boundary of the surface plasmon resonance behaves as a critical surface which accumulates the energy of plasmon-polaritons propagating in its vicinity. Let us consider a surface plasmon with a frequency just below the frequency of the surface plasmon resonance at a given location inside the droplet. Such a SP is effectively trapped inside the droplet in one of the whispering gallery modes near the critical surface, due to the fact that the effective refractive index of the droplet seen by the SP is very large [Fig. 1(c)]. The fact that surface plasmons which are localized in nanometer-scale metal particles had been previously observed in the experiment[1,2] indicates that the effective refractive index seen by the surface plasmons may reach at least $n_{eff} \sim 1000$. The fact that the droplet is large means that ray optics may be used. Since the component of the SP momentum parallel to the droplet boundary has to be conserved, such a SP will be totally internally reflected by the droplet boundary back inside the droplet at almost any angle of incidence. This is a simple consequence of the fact that at the critical boundary of the surface plasmon resonance (located just inside the droplet) the effective refractive index of the droplet as seen by the surface plasmons is infinite [according to Eq. (1), both phase and group velocity of surface plasmons is zero at surface plasmon resonance]. In addition, due to the very large density of states of the surface plasmon whispering gallery modes, even those plasmons which propagate almost perpendicular to the droplet boundary and could, in principle, be able to leave the droplet could not do it because of the surface roughness. Such plasmons would be overwhelmingly scattered into the whispering gallery modes and could not leave the droplet. On the other hand, all the incoming plasmons in this frequency range will be ''sucked'' into the whispering gallery modes of the droplet by its huge effective refractive index. Thus, the line just inside the droplet boundary where the surface plasmon resonance conditions are satisfied behaves as a critical surface. It accumulates SP's of a given resonant frequency.

We should also mentioned that the whispering gallery modes (WGM) also exist below the discussed frequency range between $\omega_p/(1+\epsilon_d)^{1/2}$ and $\omega_p/2^{1/2}$, so that the described effect is more general. However, below $\omega_p/(1+\epsilon_d)^{1/2}$ the effective refractive index experienced by surface plasmon-polaritons is of the order of 1, which makes the physical situation look more like the usual three-dimensional case. Since the properties of WGM in three dimensions are rather well established,[9] we will concentrate on the less usual case of WGM in between $\omega_p/(1+\epsilon_d)^{1/2}$ and $\omega_p/2^{1/2}$.

II. EFFECTIVE METRICS NEAR THE CRITICAL SURFACE

In principle, plasmon propagation near the critical surface may be described geometrically by an effective metric using the approach described in Ref. 3. As we will demonstrate below, the effective metric represents the distribution of surface plasmon phase velocity around the droplet in the metal plane, which may be helpful in understanding the 2D propagation properties of surface plasmons. Quantitatively the effective metric experienced by surface plasmons near the droplet boundary may be written by introducing a local slowly varying SP phase velocity $c^*(x,y) = \omega/k(x,y)$, so that the wave equation for surface plasmons may be written as

$$\left(\frac{\partial^2}{c^{*2}\partial t^2} - \frac{\partial^2}{\partial x^2} - \frac{\partial^2}{\partial y^2} \right) A = 0, \tag{2}$$

which corresponds to an effective metric

$$ds^2 = c^{*2}dt^2 - dx^2 - dy^2. \tag{3}$$

The behavior of $c^*(x,y)$ is defined by the shape and thickness of the droplet near its edge (if necessary, the droplet may be replaced by a similar shaped layer of solid dielectric), by the thickness of the metal film, and by the frequency of the surface plasmons. In order to simplify situation, let us consider a thin metal membrane with two ''linear'' droplets positioned symmetrically on both sides of the membrane [Fig. 2(a)], and assume the frequency range of incoming SP's to be small so that we can neglect the dispersion of the metal and the dielectric. The droplets thicknesses at $x=0$ correspond to the surface plasmon resonance at the illumination frequency. The droplets taper off adiabatically in positive and negative x directions on both sides of the membrane. In the

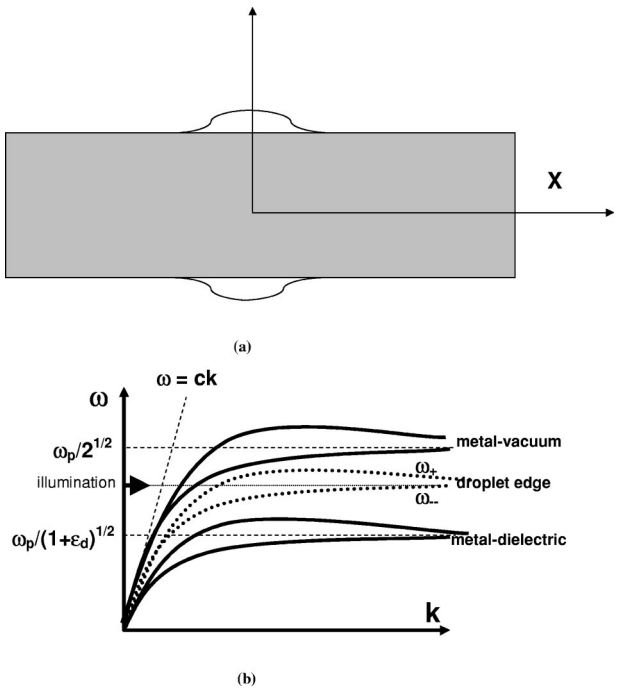

FIG. 2. (a) A thin metal membrane with two ''linear'' droplets positioned symmetrically on both sides of the membrane. The critical surface is located at $x=0$. Such geometry emulates the effective space-time geometry considered in Ref. 3. (b) Dispersion laws of the ω_- and ω_+ modes exhibit positive and negative dispersion, respectively, near the surface plasmon resonance. These branches are shown for the cases of metal-vacuum interface far from the droplets, and for the locations near $x=0$.

symmetric membrane geometry the surface plasmon spectrum consists of two branches ω_- and ω_+, which exhibit positive and negative dispersion, respectively, near the surface plasmon resonance.[4] Figure 2(b) shows the dispersion curves of both branches for the cases of metal-vacuum interface far from the droplets, and for the locations near $x=0$.

The critical surface discussed above corresponds to $c^*=0$ at $x=0$. The behavior of $c^*(x)$ near $x=0$ may be defined at will by choosing the corresponding geometry (shape and dielectric constant distribution) of the droplet edge. In order to adhere to the metric considered in Ref. 3 let us assume that $c^*=\alpha x c$ in the vicinity of $x=0$. However, we should remember that this linear behavior will be cut off somewhere near the critical surface due to such effects as Landau damping,[5] losses in the metal and the dielectric, etc. The resulting effective metric now looks like

$$ds^2=\alpha^2x^2c^2dt^2-dx^2-dy^2. \tag{4}$$

This particular choice of the shape of the droplet edge gives rise to an effective Rindler geometry.[3] Choosing a different behavior of $c^*(x)$ near $x=0$ will lead to a different effective metric. For example, the choice of $c^*=\beta x^2 c$ would produce the Reissner-Nordstrom metric near the critical surface. These various choices of the effective metric may be made possible by choosing the appropriate dielectric constant $\epsilon_d(x,y)$ and/or thickness $d(x,y)$ distribution of the absorbed layer of dielectric over the metal surface. The effects of these factors on the phase velocity of surface plasmons are complimentary to each other, which may be seen from the dispersion law of surface plasmons in a three-layer metal-dielectric-vacuum geometry described in numerous publications (see for example Ref. 2). In the limit of small plasmon phase velocities $c^*/c\ll 1$ the phase velocity can be found by solving the following nonlinear equation:

$$\frac{c^{*2}}{c^2}=\eta=\left(\frac{1}{\epsilon_d}+\frac{1}{\epsilon_m}\right)+\frac{(\epsilon_d-1)}{(\epsilon_d+1)}\left(\frac{1}{\epsilon_d}-\frac{1}{\epsilon_m}\right)\exp\left(-\frac{2\omega d}{c\,\eta^{1/2}}\right), \tag{5}$$

so that one can vary either ϵ_d or d in order to achieve the same desired phase velocity at a given frequency ω and at a given location on the metal surface. Finally, the use of optically active dielectric produces an effective Kerr metric near the critical surface as described in Ref. 6. This geometry may be quite important from the point of view of practical applications. In the frequency range where the critical surface exists only for one (left or right) kind of plasmon-polaritons, the array of such droplets will behave as a medium which exhibits giant planar optical activity. Such media are being actively developed at the moment.[7]

III. EXPERIMENTAL OBSERVATIONS OF SURFACE PLASMON WHISPERING GALLERY MODES

The surface plasmon whispering gallery modes described above are extremely easy to make and observe. In our experiments a small droplet of glycerin was placed on the gold film surface and further smeared over the surface using lens paper, so that a large number of glycerin microdroplets were formed on the surface [Fig. 3(a)]. These microdroplets were illuminated with white light through the glass prism [Fig. 1(a)] in the so-called Kretschman geometry.[2] The Kretschman geometry allows for efficient SP excitation on the gold-vacuum interface due to phase matching between the SP's and photons in the glass prism. As a result, SP's were launched into the gold film area around the droplet. Photograph taken under a microscope of one of such microdroplets is shown in Fig. 3(b). The white rim of light near the edge of the droplet is clearly seen. It corresponds to the spatial location of the surface plasmon whispering gallery modes just outside the critical surface inside the droplet, which has been described above. A small portion of the SP field has been scattered out of the two-dimensional surface plasmon world into normal three-dimensional photons. These photons produced the image in Fig. 3(b). We also conducted near-field optical measurements of the local surface plasmon field distribution around the droplet boundary Figs. 3(c), 3(d), and 3(e) using a sharp tapered optical fiber as a microscope tip. These measurements were performed similar to the measurements of surface plasmon scattering by individual surface defects described in Ref. 8. The droplet was illuminated with 488 nm laser light in the Kretschman geometry. The tip of the microscope was able to penetrate inside the glycerin droplet, and measure the local plasmon field distribution both inside and outside the droplet. Inside

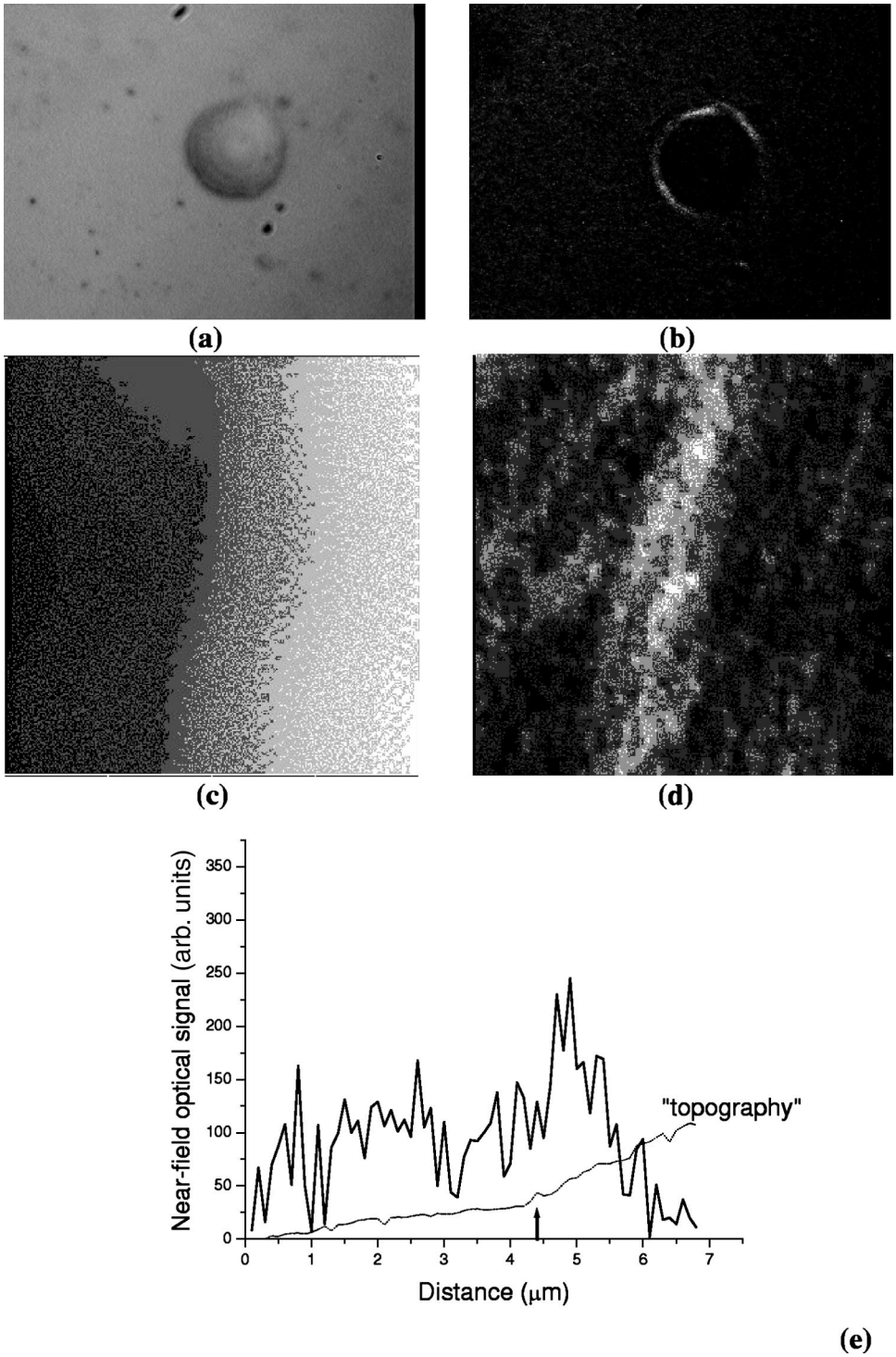

FIG. 3. Far-field (a), (b) and near-field (c), (d) images of whispering gallery modes field distribution: (a) Droplet of glycerin on a gold-film surface (illuminated from the top). The droplet diameter is approximately 15 μm. (b) The same droplet illuminated with white light in the Kretschman geometry, which provides efficient coupling of light to surface plasmons on the gold-vacuum interface [Fig. 1(a)]. The white rim around the droplet boundary corresponds to the surface plasmons trapped in the whispering gallery modes near the critical surface inside the droplet. (c) and (d) show 10×10 μm^2 topographical and near-field optical images of a similar droplet boundary (droplet is located in the right half of the images) illuminated with 488 nm laser light. Cross sections of both images are shown in (e). Position of a droplet boundary is indicated by the arrow.

the droplet (in the right half of the images) the shear-force image (c) corresponds to the increase in viscous friction rather than the droplet topography. However, this image accurately represents the location of the droplet boundary, shown by the arrow in Fig. 3(e). The sharp and narrow local maximum of the surface plasmon field just inside the droplet near its boundary is clearly visible in the near-field image Fig. 3(d) and its cross section Fig. 3(e). This feature represents the behavior of SP field near the critical surface.

We should also mention that SP's in the frequency range below $\omega_p/(1+\epsilon_d)^{1/2}$ can be excited directly inside the droplets. This might result in somewhat better coupling to whispering gallery modes. However, for most liquids in the Kretschman geometry this would require the use of prisms with much larger refractive index and illumination at much steeper angles, which could result in reduced coupling efficiency. The detailed answer to power coupling problem would require further detailed study.

The SP whispering gallery phenomenon shown in Fig. 3(b) is potentially a very interesting effect in surface plas-

mon optics. Whispering gallery modes, which are well known in the optics of light in droplets and other spherical dielectric particles, are known to substantially enhance nonlinear optical phenomena due to cavity quantum electrodynamic effects.[9] One may expect even higher enhancement of nonlinear optical mixing in liquid droplets on the metal surfaces due to enhancement of surface electromagnetic field inherent to surface plasmon excitation, and in addition, due to accumulation of SP energy near the critical surface in the vicinity of the droplet boundaries. This strong enhancement of nonlinear optical effects in liquid droplets may be very useful in chemical and biological sensing applications. It may also be responsible for the missing orders of magnitude of field enhancement in the SERS effect,[5] since various plasmon excitations are believed to play a major role in SERS.

IV. NONLINEAR OPTICS OF SURFACE PLASMON WHISPERING GALLERY MODES

The current explanation of SERS is based on the combination of electromagnetic and ''chemical'' enhancements.[5] The current calculations of the electromagnetic field enhancement take into account ''electrostatic'' field enhancement at the apices of various surface protrusions (the ''lightning rod effect''), and the local-field enhancement due to excitation of various localized surface plasmon modes in the crevices of the rough metal film. In addition, various weak and strong surface plasmon localization effects are considered in combination with the consideration of a rough metal surface as a fractal object.[10] The ''chemical'' enhancement was proposed as an explanation for the quite a few missing orders of magnitude in theoretically calculated optical-field enhancement, which follows from the magnitude of the experimentally measured SERS signals.[5] The ''chemical'' enhancement may happen if the molecular energy levels are affected by the proximity to the rough metal surface, and are drawn into resonance with the excitation field.

SERS observations are usually conducted under not so well controlled conditions when the surface topography is not well-known and ''dirty'' (the target molecules are present on the surface in random locations). On the other hand, it is well known that even monolayer surface coverages considerably shift plasmon resonance[1,2] of the metal-vacuum interface. It is reasonable to suggest that some areas of the ''dirty'' metal surface may contain compact areas covered with the multiple layers of the target or solvent molecules (even if there are no droplets on the surface). Such compact areas would affect surface plasmon propagation in a way, which is very similar to the effect of the droplets considered above: surface plasmon critical surfaces may appear near the boundaries of such areas. Experimental data shown in Fig. 3 and the theoretical arguments above strongly indicate that the local-field enhancement near these boundaries may be considerable. Even the data shown in Fig. 3(e) obtained with the limited optical resolution of the order of 100 nm[8] indicate at least ten-fold enhancement of the square of the local-field intensity near the droplet boundary. In the physical picture of surface plasmon whispering gallery modes the local SERS signal may be expected to grow by a factor of Q^2, where Q is the cavity quality factor.[9] For the surface plasmons in the visible range Q may be estimated roughly as $Q \sim L n_{eff}/\lambda$, where L is the surface plasmon free propagation length and λ is the light wavelength in vacuum. Taking into account the typical theoretical value of $L \sim 40\ \mu$m (Ref. 11) in the visible range, $Q \sim 200$ may be obtained. Thus, such surface plasmon whispering galleries may provide considerable SERS enhancements on top of the local electromagnetic enhancement due to other effects associated with the surface roughness.

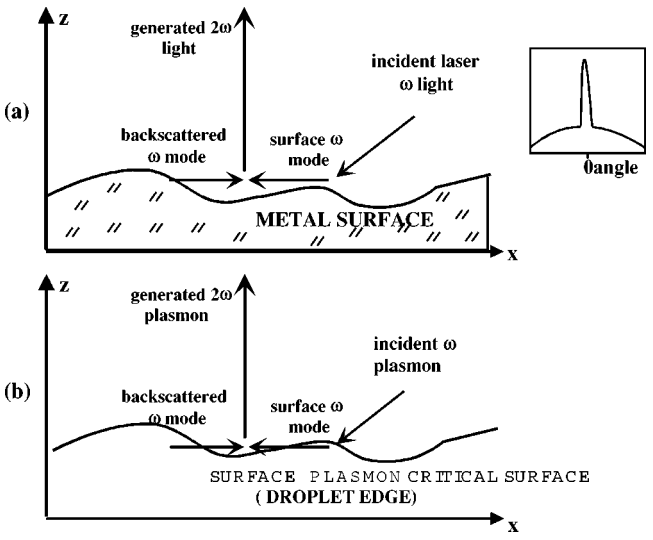

FIG. 4. (a) Strong enhancement of second harmonic emission from a randomly rough metal surface in the direction normal to the surface. A typical angular distribution of the diffuse second harmonic light is shown in the inset. (b) Second harmonic generation near the critical surface. Surface roughness is represented by a rough droplet edge. Second harmonic plasmons emitted perpendicular to the surface have the best chances to escape the droplet.

The effects of surface roughness on the properties of plasmons near the critical surface have not been considered so far. Wave propagation and localization phenomena in random media have been the topic of extensive studies during the last years.[12] One of the most striking examples of such phenomena is the strong and narrow peak of diffuse second harmonic light emission observed in the direction normal to a randomly rough metal surface [see Fig. 4(a)]. This peak is observed under the coherent illumination at any angle. This effect was initially predicted theoretically[13] and later observed in the experiment.[14] The enhanced second harmonic peak normal to the mean surface arises from the fact that a state of momentum $\mathbf{k}$ introduced into a weakly localized system will encounter a significant amount of backscattering into states of momentum centered about $-\mathbf{k}$. When these surface $\mathbf{k}$ and $-\mathbf{k}$ modes of frequency ω interact through an optical nonlinearity to generate 2ω radiative modes, the 2ω light has nonzero wave vector components only perpendicular to the mean surface. The angular width of the normal peak can be as small as a few degrees, and its amplitude far exceeds the diffuse omnidirectional second harmonic background.

Similar weak localization effects may be expected for the surface plasmon modes, which are trapped near the critical

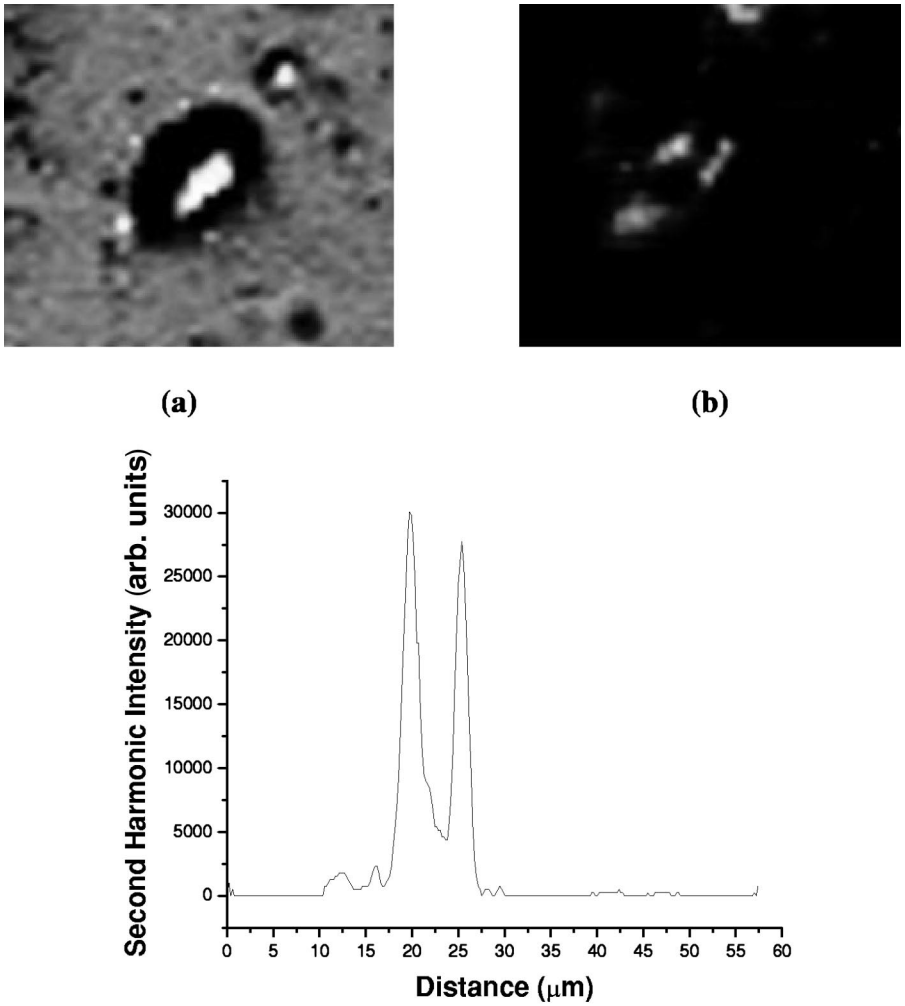

FIG. 5. (a) Microscopic image of the glycerin droplet under normal illumination. (b) SHG is seen from the droplet illuminated by 810 nm Ti:sapphire laser light in the Kretschman geometry shown in Fig. 1(a). The cross section (c) of the second harmonic image (b) indicates the droplet edge as an origin of SHG.

surface of the droplet when the metal surface exhibits moderate roughness. Similar to the case of planar rough surface,[13,14] the momentum component parallel to the edge of the droplet must be conserved in nonlinear optical processes. This means that while the surface plasmon $\mathbf{k}$ and $-\mathbf{k}$ modes of frequency ω, which interact through an optical nonlinearity, generate 2ω modes, the 2ω plasmons could have nonzero wave vector component only perpendicular to the mean edge of the droplet [Fig. 4(b)]. Thus, weak localization effects in the scattering of SP's near the critical surface should produce a pronounced peak in the angular distribution of second harmonics of plasmons in the direction normal to the droplet edge. In addition, because of such propagation direction (perpendicular to the droplet edge), these second harmonic plasmons have the best chances to escape the vicinity of the critical surface. As a result, the relative intensity of the second harmonic radiation due to the weak localization effect near the droplet edge will be much higher with respect to the diffuse second harmonic generation (SHG) than in the case of planar rough surface. The diffuse SH plasmons would remain trapped near the critical surface.

Our experiments strongly indicate enhancement of SHG near the dielectric droplets. The droplet shown in Fig. 5(a) was illuminated by the weakly focused beam (illuminated spot diameter on the order of 50 μm) from a Ti:sapphire laser system consisting of an oscillator and a regenerative amplifier operating at 810 nm (repetition rate up to 250 kHz, 100 fs pulse duration, and up to 10 μJ pulse energy), which was directed onto the sample surface in the Kretschman geometry [Fig. 1(a)]. Excitation power at the sample surface was kept below the ablation threshold of the gold film. The local SHG from the droplet illuminated by the laser can be clearly seen in Fig. 5(b), which was obtained using a far-field microscope and a charge-coupled device camera. The cross section [Fig. 5(c)] of the second harmonic image indicates the droplet edge as an origin of SHG. It should be noted, however, that while the SH frequency plasmons experience the critical surface effect near the edge of the droplet, the refractive index of glycerine is not sufficiently large for the fundamental frequency plasmons to see it. Thus, 810 nm plasmons may only be trapped into the regular whispering gallery modes near the edge of the droplet. On the other hand, the basic weak localization mechanism remains the same in the studied experimental situation.

Nonlinear optical effects put limits on the validity of the effective metrics (3) or (4). While, this statement is true in

general, it may not be valid for the lowest order nonlinearities. For example, the nonlinearities of the liquid dielectric of the form

$$\epsilon_d = \epsilon_d^{(1)} + 4\pi\chi^{(3)}E^2, \tag{6}$$

where $\epsilon_d^{(1)}$ is the linear dielectric constant, $\chi^{(3)}$ is the third-order nonlinear susceptibility of the liquid, E is the local electric field, and $\chi^{(3)}>0$, which would be responsible for the self-focusing effect in three-dimensional optics, may lead to a ''collapse'' of the surface plasmon field near the critical surface inside the droplet. This type of nonlinearity causes an effective attractive interaction of surface plasmons with each other (here we consider the case of a central-symmetric nonlinear liquid with $\chi^{(2)}=0$). Thus, we may imagine a situation where a liquid droplet is illuminated with an intense plasmon beam at a frequency below $\omega_p/(1+\epsilon_d^{(1)})^{1/2}$, so that a low-intensity plasmon field would not experience a critical surface near the droplet edge. However, the increase in the droplet refractive index due to the high-intensity plasmon field will cause the plasmon field to collapse towards an arising critical surface. Such a self-focusing effect may cause even stronger local-field enhancement. Since the effective metric describing plasmon propagation [Eqs. (3) and (4)] resembles the Rindler geometry, based on calculations in Ref. 3, one can describe the nonlinear luminescence resulting from the critical surface in this effect by an effective Hawking temperature

$$T_H = \frac{\hbar c\alpha}{\pi k_B}, \tag{7}$$

where k_B is the Boltzmann constant. For more details on the derivation of this result one may address,[3] where it is also demonstrated that cutting off c^* near $x=0$ and inclusion of the dispersion does not eliminate this radiation. In order to get a numerical estimate on this effective temperature we must assume some realistic value of α. Our approximation of a slow adiabatically changing c^* inside the droplet means that c^* does not change considerably on the scale of the local wavelength λ^* of surface plasmons. Thus, a good top estimate for α should look like $\alpha<1/\lambda\sim 1/\lambda_0$, where λ is the plasmon wavelength far from the droplet, and λ_0 is the wavelength of light in vacuum. As a result, the effective Hawking temperature of the critical surface in the described nonlinear self-focusing effect is of the order of

$$T_H \leqslant \frac{1}{2\pi^2}\frac{\hbar\omega_p}{k_B} \sim 1000 \text{ K}. \tag{8}$$

This value is reasonably large for experimental observations. This thermal radiation may be observed in a pump-probe experimental arrangement as a thermal afterglow emitted by the droplet after a short illuminating laser pulse.

The spectral range of such luminescence must be located between $\omega_p/(1+\epsilon_d)^{1/2}$ and $\omega_p/2^{1/2}$.

In conclusion, we have introduced and observed experimentally surface plasmon whispering gallery modes in liquid microdroplets on the gold-film surfaces. Behavior of surface plasmons in such geometries may be formally described using three-dimensional curved space-time metrics. Dielectric microdroplets which support whispering gallery modes are shown to exhibit strongly enhanced nonlinear optical behavior in the frequency range near the surface plasmon resonance of a metal-liquid interface. This enhancement may be responsible for the missing orders of magnitude of field enhancement in the surface enhanced Raman scattering effect.

ACKNOWLEDGMENT

This work has been supported in part by the NSF Grants Nos. ECS-0210438 and ECS-0304046.

[1] A.V. Zayats and I.I. Smolyaninov, J. Opt. A, Pure Appl. Opt. **5**, S16 (2003).
[2] H. Raether, *Surface Plasmons* (Springer, Berlin, 1988), Vol. 111.
[3] B. Reznik, Phys. Rev. D **62**, 044044 (2000).
[4] K.L. Kliewer and R. Fuchs, Phys. Rev. **144**, 495 (1966).
[5] A.G. Malshukov, Phys. Rep. **194**, 343 (1990).
[6] I.I. Smolyaninov, New J. Phys. **5**, 147.1 (2003).
[7] A. Papakostas, A. Potts, D.M. Bagnall, S.L. Prosvirnin, H.J. Coles, and N.I. Zhelude, Phys. Rev. Lett. **90**, 107404 (2003).
[8] I.I. Smolyaninov, D.L. Mazzoni, and C.C. Davis, Phys. Rev. Lett. **77**, 3877 (1996).
[9] A.J. Campillo, J.D. Eversole, and H.B. Lin, Phys. Rev. Lett. **67**, 437 (1991).
[10] V. M. Shalaev, *Nonlinear Optics of Random Media* (Springer, Berlin, 2000).
[11] P. Dawson, F. de Fornel, and J.-P. Goudonnet, Phys. Rev. Lett. **72**, 2927 (1994).
[12] A. Ishimaru, *Wave Propagation and Scattering in Random Media* (IEEE, New York, 1997).
[13] A.R. McGurn, T.A. Leskova, and V.M. Agranovich, Phys. Rev. B **44**, 11 441 (1991).
[14] O.A. Aktsipetrov, V.N. Golovkina, O.I. Kapusta, T.A. Leskova, and N.N. Novikova, Phys. Lett. A **170**, 231 (1992).